Neighborhood size effects on the evolution of cooperation under myopic dynamics

Cite as: Chaos **31**, 123113 (2021); doi: 10.1063/5.0073632
Submitted: 1 October 2021 · Accepted: 23 November 2021 ·
Published Online: 8 December 2021

Juan Shi,[1,2] Jinzhuo Liu,[3] Matjaž Perc,[4,5,6,7] Zhenghong Deng,[1,a)] and Zhen Wang[2,b)]

AFFILIATIONS

[1]School of Automation, Northwestern Polytechnical University, Shaanxi 710072, China
[2]School of Artificial Intelligence, Optics and Electronics (iOPEN), Northwestern Polytechnical University, Shaanxi 710072, China
[3]School of Software, Yunnan University, Kunming, Yunnan 650504, China
[4]Faculty of Natural Sciences and Mathematics, University of Maribor, Koroška cesta 160, 2000 Maribor, Slovenia
[5]Department of Medical Research, China Medical University Hospital, China Medical University, Taichung 404332, Taiwan
[6]Alma Mater Europaea, Slovenska ulica 17, 2000 Maribor, Slovenia
[7]Complexity Science Hub Vienna, Josefstädterstraße 39, 1080 Vienna, Austria

[a)]dthree@nwpu.edu.cn
[b)]**Author to whom correspondence should be addressed:** w-zhen@nwpu.edu.cn

ABSTRACT

We study the evolution of cooperation in 2×2 social dilemma games in which players are located on a two-dimensional square lattice. During the evolution, each player modifies her strategy by means of myopic update dynamic to maximize her payoff while composing neighborhoods of different sizes, which are characterized by the corresponding radius, r. An investigation of the sublattice-ordered spatial structure for different values of r reveals that some patterns formed by cooperators and defectors can help the former to survive, even under untoward conditions. In contrast to individuals who resist the invasion of defectors by forming clusters due to network reciprocity, innovators spontaneously organize a socially divisive structure that provides strong support for the evolution of cooperation and advances better social systems.

As a basic research issue, how to maintain high-level cooperation has attracted great attention both theoretically and experimentally. The most commonly used theoretical framework to study the cooperation between selfish individuals is evolutionary game theory. Here, we study the effects of myopic strategy update and neighborhood on social dilemma games. Interestingly, the evolution outcomes show a spatial order strategy distribution, which is similar to the antiferromagnetic order in the spin system. In detail, below the threshold temptation value, the distribution of cooperators is homogeneous; i.e., $\rho_A = \rho_B$. While above the threshold value, there is an ordered structure. That is, one sublattice is mainly occupied by defectors and the other sublattice is occupied by cooperators. This orderly arrangement of cooperators and defectors can provide maximum total payoff in social dilemmas. Through mean-field approximation and Monte Carlo simulation, we associate the emergence of these ordered structures with the microscopic dynamics of the evolutionary process.

I. INTRODUCTION

In the past half century, cooperation among individuals for the benefit of others has been a subject of interest in the natural and social sciences.[1,2] Evolutionary game theory is often used as a theoretical framework to understand and explain the evolution of cooperation,[3–5] and the prisoner's dilemma (PD) game is frequently used for theoretical analysis.[6–12] In the PD game, two players can either cooperate (C) or defect (D). The two players both receive R (reward) if they mutually cooperate and P (punishment) after a mutual defection. If a defector exploits a cooperator, the defector receives T (temptation), and the cooperator receives a small payoff, S (sucker). In the PD game, the rank of the four payoff values is $T > R > P > S$ and $2R > T + S$. The only Nash equilibrium for the PD game is the pure strategy (D, D). In a population in which all individuals interact with each other, both players have made the choice that seems to be in their best interest, but in fact, they have fallen into a dilemma that is not beneficial for either side. There is

a contradiction between personal interest and collective interests in that individuals making rational choices often lead to collective irrationality. Therefore, how to promote cooperative strategies among selfish participants has always been a hot research topic.[13–18]

The spatial structure introduced by Nowak and May inspired follow-up work and enabled cooperators to aggregate compact clusters on the structured network to protect themselves against invading defectors.[19] A series of subsequent studies placed evolutionary games in regular networks,[20–22] small-world networks,[23,24] scale-free networks,[25,26] and other related network topologies.[27–29] In addition to network reciprocity, various mechanisms, such as kin selection,[30] direct reciprocity,[31] indirect reciprocity,[32] and group selection,[33] can be used to simulate the emergence of cooperative behaviors and explain the causes of cooperation. In line with these achievements, different real-world natural mechanisms have also been explored in structured populations to explain cooperative behaviors, for example, punishment,[34,35] teaching activity,[36] reputation,[37,38] social diversity,[39,40] aspiring to be the fittest,[41,42] and noise,[43,44] to name but a few.[45–47]

Recently, the myopic rule has attracted considerable attention.[48–57] Compared to imitation of a better-performing neighbor, the myopic rule is more consistent with the innovative characteristics of human beings.[58,59] For the imitation update rule, the player can choose only a strategy owned by the neighbor; as a result, if a strategy disappears, it will not appear again.[49,55–57] However, the myopic rule allows players to make different choices than their neighbors. In the present work, inspired by previous works[52–55] that investigated the consequences of a structured population for myopic players with specific properties, we study the myopic dynamical rule that exhibits different disordered and sublattice-ordered spatial arrangements when the number of interactional neighbors is increased. We explore the effects of neighborhood size on 2×2 social dilemma games [including prisoner's dilemma (PD), snowdrift (SD), stag-hunt (SH), and the harmony game (HG)] with myopic players located on a square lattice.[60,61] By using the Monte Carlo (MC) method to simulate evolutionary dynamics, we observe an interesting phenomenon: as the number of neighbors increases, the cooperators and defectors on the square lattice form different special ordered structures. This phenomenon also corresponds to real-world society, in which individuals occupy a position in a complex social relation, thus forming different role relations and special structures. It is worth mentioning that the mean-field approximation provides a simple explanation of this phenomenon.

The remainder of this paper is arranged as follows. We first introduce the model. Subsequently, we investigate the effects of different neighborhood sizes both by mean-field theory and by MC simulations. Then, we use the local pattern steady-state analysis to explain the spatial structure of different strategy distributions. Finally, we summarize our conclusions and discuss potential directions for future research.

II. MODEL

We study the evolution of cooperation in 2×2 games on a square lattice with $N = L \times L$ sites and periodic boundary conditions. Every site is initially assigned with a player that can be, with equal probability, either a cooperator (C) or a defector (D) and represented by the variable S_i, $i = 1, \ldots, N$. Different interaction ranges can be explored by considering regions that go beyond the standard von Neumann neighborhood around the focal site [Fig. 1(a)]. Here, we include all the $N_r = 2r(r+1)$ sites that can be reached within r steps. Figure 1 illustrates the increasing neighborhood sizes corresponding to $r = 1$ (a), 2 (b), and 3 (c). The payoff received by a player when interacting with a neighbor depends on their strategies and is obtained from the matrix

$$\begin{array}{cc} & \begin{array}{cc} \mathrm{C} & \mathrm{D} \end{array} \\ \begin{array}{c} \mathrm{C} \\ \mathrm{D} \end{array} & \begin{pmatrix} R & S \\ T & P \end{pmatrix}. \end{array} \tag{1}$$

The elements of the payoff matrix are rescaled such that $R = 1$, $P = 0$, $T \in [0, 2]$, and $S \in [-1, 1]$. Depending on the chosen range for the sucker's payoff S and the temptation T, four different dilemmas are obtained: (a) prisoner's dilemma (PD) game when $S < 0$ and $T > 1$, (b) snowdrift (SD) game when $S > 0$ and $T > 1$, (c) the stag-hunt (SH) game when $S < 0$ and $T < 1$, and the harmony

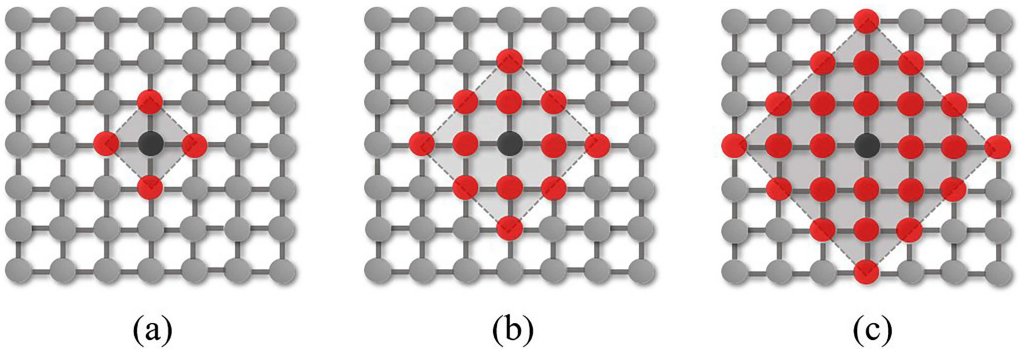

FIG. 1. Examples of different neighborhoods for the square lattice. Starting at the focal player (black dot), N_r sites can be reached within r steps. From (a) to (c): $r = 1$ (von Neumann), 2, and 3, corresponding to $N_r = 4$, 12, and 24, respectively. Notice that the Moore neighborhood is intermediate between $r = 1$ and 2.

game (HG) when $S > 0$ and $T < 1$.[62,63] The dynamics uses an asynchronous Monte Carlo (MC) procedure as follows. First, a randomly selected player i with strategy S_i accumulates the total payoff P_i by interacting with all its neighbors (those that are within r steps). Next, the payoff P_i is compared with what would have been obtained (P_i') with a different strategy, S_i', with the same neighbors. Accordingly with the myopic rule, the player updates its strategy with probability

$$p(S_i' \rightarrow S_i) = \frac{1}{1+\exp\left(\frac{P_i - P_i'}{K}\right)}. \quad (2)$$

Through simulation, we found that when K is greater than 0.2, there will be an ordered structure in the snowdrift (SD) game. In the literature,[52–54] K is usually set between [0.001, 0.4] to simulate minor irrationalities. Therefore, the amplitude of noise is set to $K = 0.25$ (its inverse, $1/K$, is called the intensity of selection). For the sake of comparison, the imitation updating rule is also considered, where the focal player i updates its strategy by randomly choosing a neighbor j (with payoff P_j) and adopting its strategy with the probability,[64]

$$p(S_j \rightarrow S_i) = \frac{1}{1+\exp\left(\frac{P_i - P_j}{K}\right)}. \quad (3)$$

The amount of cooperation is measured by the average fraction of cooperators in the system, ρ. In order to check whether staggered ordering (similar to an antiferromagnet) is possible, the square lattice is divided into two sublattices (A and B) in a checkerboard pattern. The fraction of cooperators in each sublattice is thus represented by ρ_A and ρ_B, respectively. Within the range r, the number of sites in each sublattice is N_A and N_B such that $N_A + N_B = N_r = 2r(r+1)$. For r odd, there is $N_A = r^2 - 1$ and $N_B = (r+1)^2$ sites around a focal site in sublattice A. For r even, $N_A = r(r+2)$ and $N_B = r^2$. If the focal site is in the sublattice B, we switch the roles of both indices in the above expressions.

The results of the MC simulations presented below were typically obtained for $L = 400$. We checked, through larger system sizes (up to $L = 2000$), that finite-size effects are not significative. To assure that the system reached a stationary state, the first 10^4–10^6 MCS (one Monte Carlo Step, MCS, corresponds to N site updatings) were discarded. The results shown are averages over 100 independent samples for each set of parameters (unless indicated, the error bars are smaller than the symbol sizes).

III. RESULT AND ANALYSIS

The myopic model is first analyzed using a mean-field approximation for neighborhoods of different radii r. For simplicity, we choose a weak PD game version (namely, $S = 0$) and study the role of the temptation T. Playing with all its $N_r = 2r(r+1)$ neighbors (n of which are cooperators, with $0 \le n \le N_r$), a cooperative player would obtain the payoff $P^{(C)} = n$, while a defector would get $P^{(D)} = nT$. The agent tries to optimize its payoff using Eq. (2). The temporal evolution for the density of cooperators ρ is given by

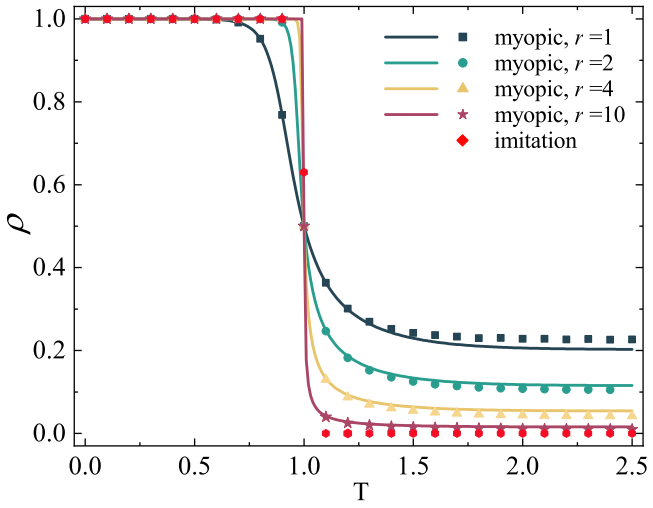

FIG. 2. Average fraction of cooperators ρ for the weak version ($S = 0$) of the PD game as a function of temptation to defect T and different values of r. The mean-field predictions, obtained from the numerical solution of Eq. (4), are shown as continuous lines and compared with the MC simulations (points) on the square lattice with $K = 0.25$ and $L = 400$. For the imitation rule, cooperation vanishes when temptation is small ($T = 1.04$). Nonetheless, regardless the value of r, the myopic rule always presents a residual level of cooperation as cooperators resist to be completely invaded by defectors.

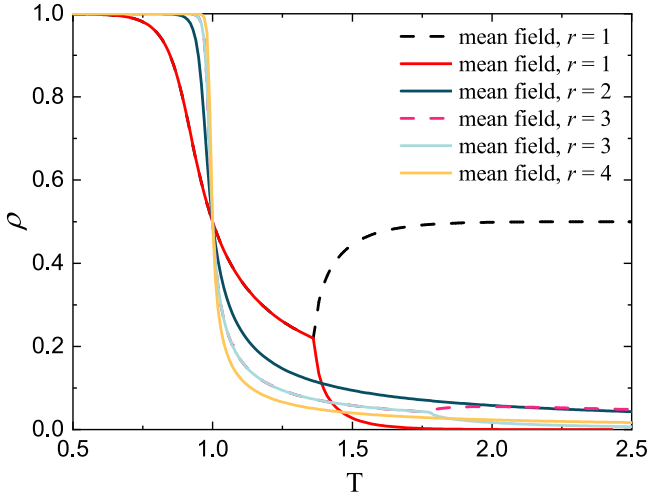

FIG. 3. Fraction of cooperation in the sublattices (ρ_A and ρ_B) as a function of temptation to defect T for different values r, predicted by mean-field theory for the weak PD game ($S = 0$) on square lattices at $K = 0.25$.

$$\dot{\rho} = \sum_{n=0}^{N_r} \binom{N_r}{n} \rho^n (1-\rho)^{N_r-n} \left[-\frac{\rho}{1+\exp\left(\frac{n(1-T)}{K}\right)} + \frac{1-\rho}{1+\exp\left(-\frac{n(1-T)}{K}\right)} \right]$$
$$= \sum_{n=0}^{N_r} \binom{N_r}{n} \rho^n (1-\rho)^{N_r-n} \left[\frac{1}{1+\exp\left(-\frac{n(1-T)}{K}\right)} - \rho \right]. \quad (4)$$

The above MF equation can be numerically solved, and the fixed points, which indicate the asymptotic fraction of cooperators, are shown in Fig. 2 (continuous lines) for different values of r. For $T > 1$, $r = 1$ presents the largest amount of cooperation with the myopic updating rule, and the larger r is, the steeper the curve becomes and ρ gradually decreases. Notice that a residual level of cooperation remains within the population, which is approximately independent of the value of the temptation, even when the environment is very hostile (large values of T), a well known property of the myopic rule.[60] These MF predictions are also observed in the MC simulations, Fig. 2 (points), and the comparison shows a very good agreement. Interestingly, as the size of the neighborhood increases, the amount of cooperation decreases. With an enlarged neighborhood, the cooperators forming a sustainable cluster do not need to be nearest neighbors and some of these clusters always persist. However, more neighbors are also helpful to defectors, and the number of cooperators decreases. For comparison, we also considered the imitation dynamics, Eq. (3), where the strategy of the player can be inherited from a random neighbor depending on their relative payoffs. In this case, already for $r = 1$, the fraction of cooperators quickly decreases to zero at $T = 1.04$, as depicted in Fig. 2 (red points).

Previous results for the particular case $r = 1$[52] have shown, in some cases, particular spatial structures, akin to an antiferromagnetic ordering. Indeed, dividing the system into two sublattices, A and B, it was remarked that in some situations, their occupation by cooperators becomes asymmetric. We then extend the above analysis to investigate whether such sublattice symmetry breaking occurs also at the MF level for different r values. The payoff of cooperators and defectors in sublattice A (for B, switch all A and B labels) can be approximated, when r is odd, by

$$P_A^{(C)} = (r+1)^2[R\rho_B + S(1-\rho_B)] + (r^2-1)[R\rho_A + S(1-\rho_A)],$$
$$P_A^{(D)} = (r+1)^2[T\rho_B + P(1-\rho_B)] + (r^2-1)[T\rho_A + P(1-\rho_A)] \quad (5)$$

and, when r is even, by

$$P_A^{(C)} = r^2[R\rho_B + S(1-\rho_B)] + r(r+2)[R\rho_A + S(1-\rho_A)],$$
$$P_A^{(D)} = r^2[T\rho_B + P(1-\rho_B)] + r(r+2)[T\rho_A + P(1-\rho_A)]. \quad (6)$$

In the following, we set $R = 1$ and $P = 0$.

Based on the myopic strategy updating rule, we obtain the following equation for the time derivative of cooperation frequency on sublattice A:

$$\dot{\rho}_A = -\rho_A \frac{1}{1+\exp\frac{P_A^{(C)}-P_A^{(D)}}{K}} + (1-\rho_A)\frac{1}{1+\exp\frac{P_A^{(D)}-P_A^{(C)}}{K}}. \quad (7)$$

By combining expression (5) and Eq. (7), we obtain the equations for the fraction of cooperators on sublattices A and B for different r values. When r is odd,

$$\dot{\rho_A} = \frac{1}{1+\exp\left\{\left\{(r+1)^2\left[(S+T-R-P)\,\rho_B - S + P\right] + (r^2-1)\left[(S+T-R-P)\,\rho_A - S + P\right]\right\}/K\right\}} - \rho_A, \quad (8)$$

$$\dot{\rho_B} = \frac{1}{1+\exp\left\{\left\{(r+1)^2\left[(S+T-R-P)\,\rho_A - S + P\right] + (r^2-1)\left[(S+T-R-P)\,\rho_B - S + P\right]\right\}/K\right\}} - \rho_B. \quad (9)$$

When r is even,

$$\dot{\rho_A} = \frac{1}{1+\exp\left\{\left\{r^2\left[(S+T-R-P)\,\rho_B - S + P\right] + r\,(r+2)\left[(S+T-R-P)\,\rho_A - S + P\right]\right\}/K\right\}} - \rho_A, \quad (10)$$

$$\dot{\rho_B} = \frac{1}{1+\exp\left\{\left\{r^2\left[(S+T-R-P)\,\rho_A - S + P\right] + r\,(r+2)\left[(S+P-R-T)\,\rho_B - S + P\right]\right\}/K\right\}} - \rho_B. \quad (11)$$

Figure 3 shows the results of the mean-field prediction of the fraction of cooperation in the sublattices as a function of temptation for various radii r. When $r = 1$, the distribution of cooperators is homogeneous below the threshold of temptation to defect b ($\rho_A = \rho_B$). As the temptation value increases, the mean-field theory predicts a long-range ordered state ($\rho_A = 0, \rho_B = 0.5$). Interestingly, when $r = 2$, regardless of the temptation value, the phenomenon of sublattice ordering disappears. Specifically, the distribution of cooperators in sublattices A and B is always homogeneous ($\rho_A = \rho_B$). For $r = 3$, the phenomenon of sublattice ordering emerges again; however, the difference between the frequency of cooperation in the two sublattices is much less than that of $r = 1$. For $r = 4$, similar to $r = 2$, the sublattice ordering structure disappears. When $r > 4$, the cooperative distribution of the two sublattices will converge, regardless of the value of r.

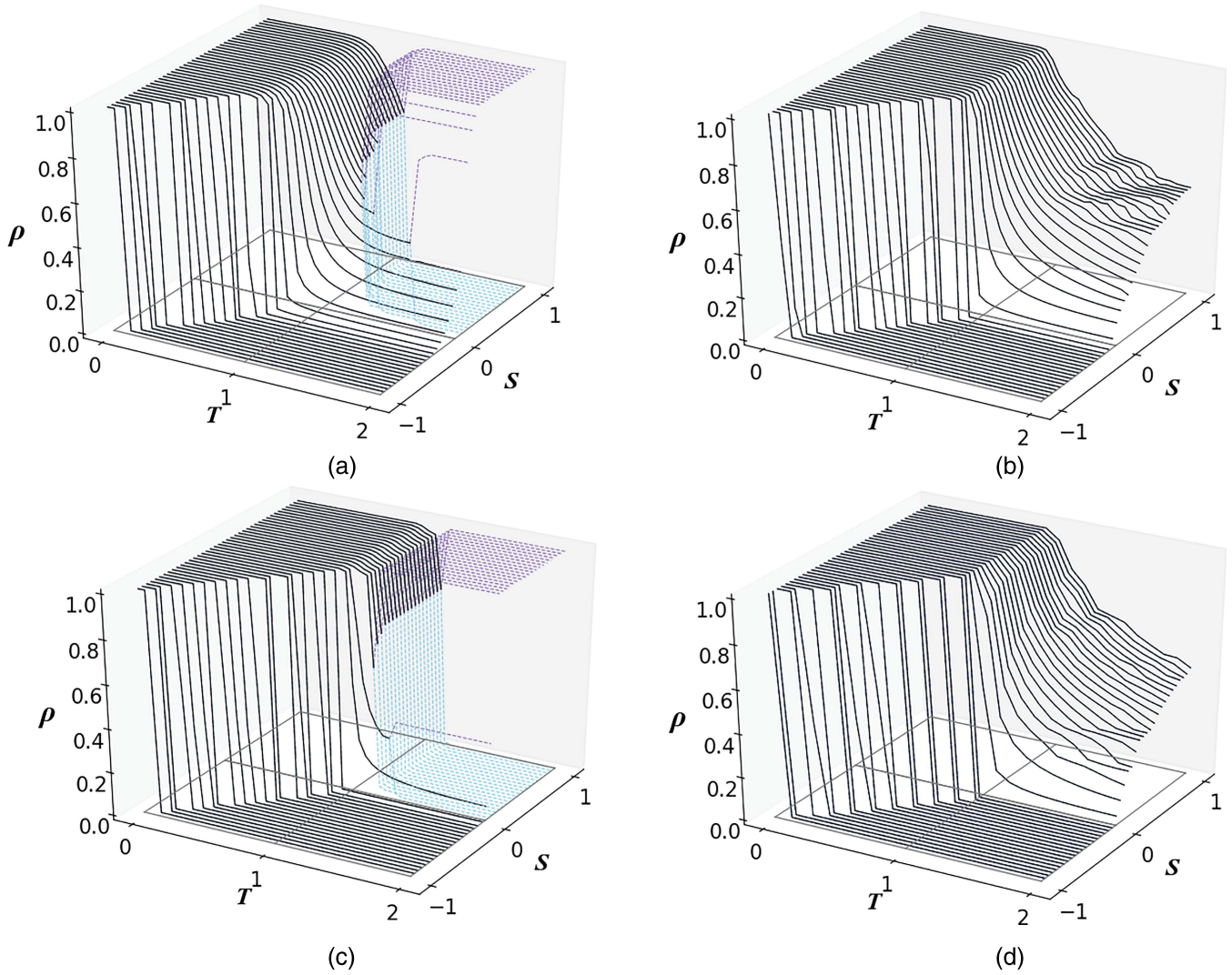

FIG. 4. Frequency of cooperation in the sublattices (ρ_A and ρ_B) when varying T and S for $K = 0.25$. From (a) to (d), the values of r are 1, 2, 3, and 4, respectively. The solid lines indicate that the fraction of cooperation in sublattices A and B is nearly equal; that is, they show the absence of sublattice ordering. The dashed lines indicate sublattice ordering patterns.

Next, we use MC simulation to verify the prediction of the mean-field theory. For different radii r, the results of the MC simulations are summarized in Fig. 4, where we can distinguish two types of ordered structures. Note that all cases differ mainly in the SD regions and that the above-mentioned sublattice ordering occurs within the range of the SD game. The dynamics evolve in almost the same way in the PD, HG, and SH regions.

To determine why different values of r lead to different results for the evolution of cooperation, in Fig. 5, we show snapshots of the MC steps 0, 100, 10 000, and 39 999 for the four scenarios ($r = 1$, 2, 3, and 4) on the SD region. In all cases, cooperators are depicted as blue, while defectors are depicted as red. Interestingly, different r values lead to spatial patterns with typical characteristics. As shown in Figs. 5(a)–5(d), where $r = 1$, multiple "lines" emerge in the checkerboard background. As the system evolves, the "line" gradually decreases, eventually forming a black-and-white checkerboard format in which one sublattice is occupied only by the cooperators ($\rho_A = 1$), while the other is occupied by the defectors ($\rho_B = 0$). For $r = 2$ [Fig. 5(b)], a checkerboard-like pattern is formed by glancing at the diagram, but the organization of cooperators and defectors is totally different from that for $r = 1$. In fact, the blue point in Fig. 5(h) is a 2×2 cooperator cluster. In addition, the fraction of cooperation is equal on the two sublattices ($\rho_A = \rho_B$). For $r = 3$, when the system evolves to a stable state, it is

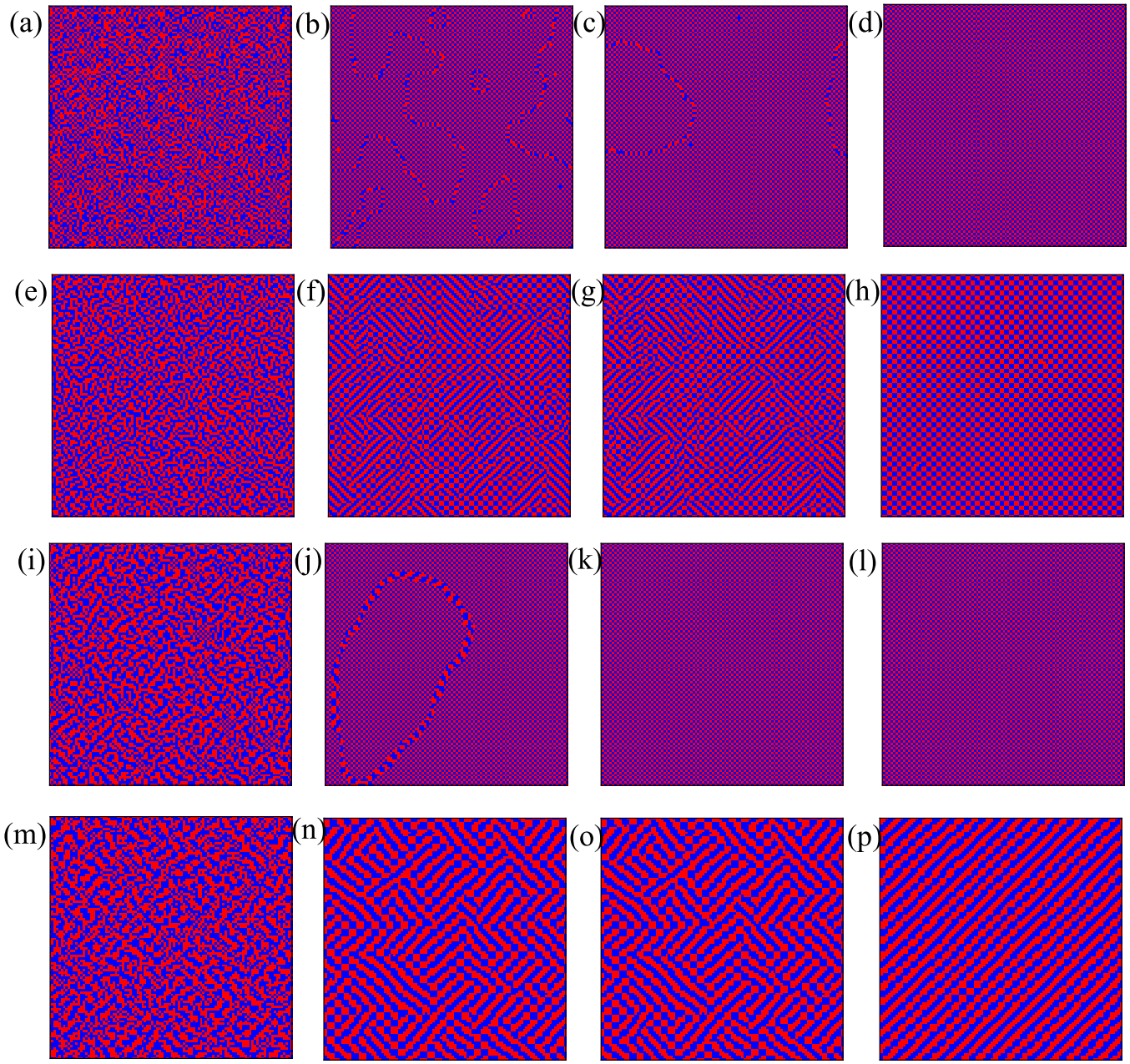

FIG. 5. The distribution of strategy from a random initial state in Monte Carlo steps 0, 100, 10 000, and 39 999 (left to right) for r = 1 (a)–(d), r = 2 (e)–(h), r = 3 (i)–(l), and r = 4 (m)–(p). Cooperators and defectors are represented by blue and red, respectively. All panels are depicted on a 100 × 100 spatial lattice. All results are obtained for $T = 1.5$ and $S = 0.5$.

similar to $r = 1$; that is, it evolves to a checkerboard pattern ($\rho_A = 1$, $\rho_B = 0$). The steady state formed for $r = 4$ is different from the previous steady states, as it is in the shape of bars. However, it can be observed that each cooperator (defector) has the same pattern of strategies in her neighborhood for a certain r. Compared to the imitation update rule, which allows cooperators to prevent defectors by forming giant clusters, the myopic update rule brings an innovative dynamic that makes cooperators maintain cooperation by forming a special pattern of strategies. In human society, although solidarity can have a great impact on cooperation, the social division

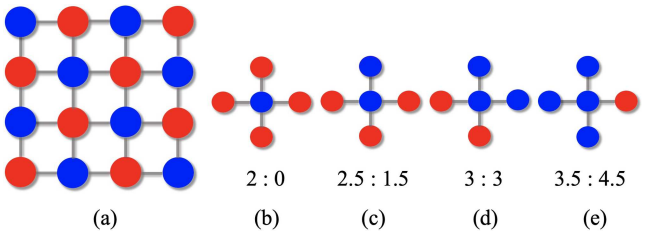

FIG. 6. Local spatial patterns in the sublattice-ordered arrangement of defectors and cooperators for $r = 1$. A blue circle indicates a cooperator, and a red circle indicates a defector. (a) shows the pattern of the system evolving to a stable state. (b)–(e) are some strategy distribution patterns that appear in the system during the evolution process.

in which each individual plays a certain role can produce a greater collective benefit.

Finally, to further explain why different r values lead to different special spatial structures, we analyze the stability of the ordered arrangement of strategies under the microscopic perspective. The ratio in Fig. 6 represents the payoff ratio of the focal player if he chooses both cooperation and defection ($W_C : W_D$) in the case of the neighbors being unchanged. Figure 6(b) is obviously the most stable pattern with the highest payoff ratio. Meanwhile, the pattern opposite to Fig. 6(a), that is, four cooperators around the defector (not shown in the figure), is also stable for a reason similar to that for Fig. 6(a). Figure 7(a) shows the pattern of the system evolving to a stable state when $r = 2$. Figures 7(b) and 7(c) show the two different patterns when $r = 2$, which are different from the pattern when the system is stable. In contrast to Fig. 6(a), every four players with the same strategy form a 2×2 cluster, while four clusters with opposite strategies are located around the former clusters. Figure 7(a) shows the pattern of the system evolving to a stable state in which the diamond-shaped shadows represent the neighborhoods of the focal players C1, C2, C3, and C4. Figures 7(b) and 7(c) present two other possible patterns. Since each akin player should have the same pattern of strategies in her neighborhood, some specific patterns are removed, such as the pattern of a cooperator surrounded by 12 defectors. Compared to the patterns presented in Figs. 7(b) and 7(c), the pattern in Fig. 7(a) gives cooperators the highest payoff ratio and spontaneously remains stable. In the case of $r = 3$, because akin players should have the same pattern of strategies in their neighborhoods, individuals cannot form 3×3 clusters with the same strategies. The checkerboard pattern is the only one that can be formed when the system is stable. When r is greater than or equal to 4, the stable patterns can be explained similarly.

IV. CONCLUSION

Our model is motivated by human society, in which players who are innovative are able to choose strategies that are not within their neighborhood. To explore and quantify the consequence of innovation dynamics in the context of different numbers of neighbors, we use MC simulation and mean-field theory to identify this model. Interestingly, when $r = 1$ and $r = 3$, an ordered spatial strategy distribution emerges ($\rho_A = 0$, $\rho_B = 1$), which is analogous to a checkboard pattern and enables the cooperators to effectively resist the invasion of defectors. When $r = 2$ and $r = 4$, the phenomenon of the ordering structure disappears ($\rho_A = \rho_B$), and the special spatial structure of the system enables the cooperators to survive. By investigating the reasons for the special strategy distribution, we use a microscopic perspective to analyze the local pattern in the stable state of the system. We find that each player with the same strategy has the same neighborhood structure. Therefore, there is a special role separation between the cooperator and the defector. In contrast to cooperators forming huge cooperative clusters to resist the invasion of defectors under the imitation dynamic, cooperators survive by forming some special patterns in which cooperators and defectors live together with a certain order under a myopic dynamic. The social division assigns different characters to different members of the society, and a reasonable social structure can lead to social

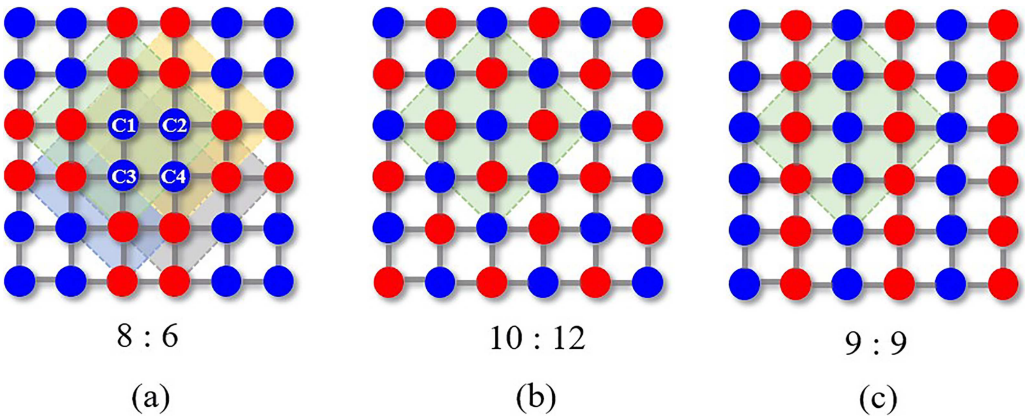

FIG. 7. Local spatial patterns in the sublattice-ordered arrangement of defectors and cooperators for $r = 2$. The colors and other details are the same as in Fig. 6(a) depicts the steady state at $r = 2$, and the four shaded rhomboids in (a) represent the domains of the player's neighbors centered on C1, C2, C3, and C4. (b) and (c) are the patterns that explain why (a) is the final steady state of the system when $r = 2$. The shaded rhomboids in (b) and (c) represent the domains of the player's neighbors.

development. Our work may be meaningful for understanding the impact of social division on the level of cooperation with different neighborhood sizes.

ACKNOWLEDGMENTS

We thank Jeferson Arenzon for useful suggestions and discussion. We acknowledge support from the National Natural Science Foundation for Distinguished Young Scholars (Grant No. 62025602), the National Natural Science Foundation of China (NNSFC) (Grant Nos. U1803263, 11931015, 81961138010, 1302267, 11161053, 61662085, 61462092, and 61866039), the National Key R&D Program of China (No. 2018YFB1403501), the National Key R&D Program of China (No. 2019YFB2102304), the Fok Ying-Tong Education Foundation, China (No. 171105), the Key Technology Research and Development Program of Science and Technology—Scientific and Technological Innovation Team of Shaanxi Province (Grant No. 2020TD-013), the Key Area R&D Program of Guangdong Province (No. 2019B010137004), the Science Foundation of Yunnan Province Education Department (Grant No. 2017ZZX08), the science and technology innovative research team of Yunnan Province (Grant No. 2017HC012), the Natural Science Foundation of Yunnan Province (Grant No. 2019FB083), and the Slovenian Research Agency (Grant Nos. P1-0403 and J1-2457).

AUTHOR DECLARATIONS

Conflict of Interest

The authors have no conflicts to disclose.

DATA AVAILABILITY

The data that support the findings of this study are available from the corresponding author upon reasonable request.

REFERENCES

[1]R. Axelrod and W. D. Hamilton, "The evolution of cooperation," Science **211**, 1390–1396 (1981).
[2]E. Pennisi, "How did cooperative behavior evolve?," Science **309**, 93 (2005).
[3]J. M. Smith, *Evolution and the Theory of Games* (Cambridge University Press, 1982).
[4]J. W. Weibull, *Evolutionary Game Theory* (MIT Press, 1997).
[5]J. Hofbauer, K. Sigmund *et al.*, *Evolutionary Games and Population Dynamics* (Cambridge University Press, 1998).
[6]G. Szabó and C. Tőke, "Evolutionary prisoner's dilemma game on a square lattice," Phys. Rev. E **58**, 69 (1998).
[7]G. Abramson and M. Kuperman, "Social games in a social network," Phys. Rev. E **63**, 030901 (2001).
[8]F. C. Santos and J. M. Pacheco, "Scale-free networks provide a unifying framework for the emergence of cooperation," Phys. Rev. Lett. **95**, 098104 (2005).
[9]C. Chu, C. Mu, J. Liu, C. Liu, S. Boccaletti, L. Shi, and Z. Wang, "Aspiration-based coevolution of node weights promotes cooperation in the spatial prisoner's dilemma game," New J. Phys. **21**, 063024 (2019).
[10]C. Shen, C. Chu, L. Shi, M. Perc, and Z. Wang, "Aspiration-based coevolution of link weight promotes cooperation in the spatial prisoner's dilemma game," R. Soc. Open Sci. **5**, 180199 (2018).
[11]C. Chu, Y. Zhai, C. Mu, D. Hu, T. Li, and L. Shi, "Reputation-based popularity promotes cooperation in the spatial prisoner's dilemma game," Appl. Math. Comput. **362**, 124493 (2019).
[12]C. Hilbe, Š. Šimsa, K. Chatterjee, and M. A. Nowak, "Evolution of cooperation in stochastic games," Nature **559**, 246–249 (2018).
[13]C. Zhu, S. Sun, L. Wang, S. Ding, J. Wang, and C. Xia, "Promotion of cooperation due to diversity of players in the spatial public goods game with increasing neighborhood size," Physica A **406**, 145–154 (2014).
[14]K. Donahue, O. P. Hauser, M. A. Nowak, and C. Hilbe, "Evolving cooperation in multichannel games," Nat. Commun. **11**, 3885 (2020).
[15]C. Xia, Q. Miao, and J. Zhang, "Impact of neighborhood separation on the spatial reciprocity in the prisoner's dilemma game," Chaos, Solitons Fractals **51**, 22–30 (2013).
[16]M. Diakonova, V. Nicosia, V. Latora, and M. San Miguel, "Irreducibility of multilayer network dynamics: The case of the voter model," New J. Phys. **18**, 023010 (2016).
[17]K.-K. Kleineberg, "Metric clusters in evolutionary games on scale-free networks," Nat. Commun. **8**, 1 (2017).
[18]J. Wang, C. Xia, Y. Wang, S. Ding, and J. Sun, "Spatial prisoner's dilemma games with increasing size of the interaction neighborhood on regular lattices," Chin. Sci. Bull. **57**, 724–728 (2012).
[19]M. A. Nowak and R. M. May, "Evolutionary games and spatial chaos," Nature **359**, 826–829 (1992).
[20]D. Jia, T. Li, Y. Zhao, X. Zhang, and Z. Wang, "Empty nodes affect conditional cooperation under reinforcement learning," Appl. Math. Comput. **413**, 126658 (2022).
[21]Z. Song, H. Guo, D. Jia, M. Perc, X. Li, and Z. Wang, "Third party interventions mitigate conflicts on interdependent networks," Appl. Math. Comput. **403**, 126178 (2021).
[22]D. Jia, X. Wang, Z. Song, I. Romić, X. Li, M. Jusup, and Z. Wang, "Evolutionary dynamics drives role specialization in a community of players," J. R. Soc. Interface **17**, 20200174 (2020).
[23]D. J. Watts and S. H. Strogatz, "Collective dynamics of 'small-world' networks," Nature **393**, 440–442 (1998).
[24]B. J. Kim, A. Trusina, P. Holme, P. Minnhagen, J. S. Chung, and M. Choi, "Dynamic instabilities induced by asymmetric influence: Prisoners' dilemma game in small-world networks," Phys. Rev. E **66**, 021907 (2002).
[25]C. P. Warren, L. M. Sander, and I. M. Sokolov, "Geography in a scale-free network model," Phys. Rev. E **66**, 056105 (2002).
[26]S. Fortunato, A. Flammini, and F. Menczer, "Scale-free network growth by ranking," Phys. Rev. Lett. **96**, 218701 (2006).
[27]K. Huang, Z. Wang, and M. Jusup, "Incorporating latent constraints to enhance inference of network structure," IEEE Trans. Netw. Sci. Eng. **7**, 466–475 (2018).
[28]K. Huang, S. Li, P. Dai, Z. Wang, and Z. Yu, "SDARE: A stacked denoising autoencoder method for game dynamics network structure reconstruction," Neural Netw. **126**, 143–152 (2020).
[29]K. Huang, Z. Xiang, W. Deng, C. Yang, and Z. Wang, "False data injection attacks detection in smart grid: A structural sparse matrix separation method," IEEE Trans. Netw. Sci. Eng. **8**, 2545–2558 (2021).
[30]W. D. Hamilton, "The genetical evolution of social behaviour. II," J. Theor. Biol. **7**, 17–52 (1964).
[31]R. L. Trivers, "The evolution of reciprocal altruism," Q. Rev. Biol. **46**, 35–57 (1971).
[32]M. A. Nowak, "Five rules for the evolution of cooperation," Science **314**, 1560–1563 (2006).
[33]D. S. Wilson, "Structured demes and the evolution of group-advantageous traits," Am. Nat. **111**, 157–185 (1977).
[34]J. Li, Y. Liu, Z. Wang, and H. Xia, "Egoistic punishment outcompetes altruistic punishment in the spatial public goods game," Sci. Rep. **11**, 1 (2021).
[35]S. Podder, S. Righi, and F. Pancotto, "Reputation and punishment sustain cooperation in the optional public goods game," Philos. Trans. R. Soc., B **376**, 20200293 (2021).
[36]A. Szolnoki and M. Perc, "Coevolution of teaching activity promotes cooperation," New J. Phys. **10**, 043036 (2008).
[37]Q. Jian, X. Li, J. Wang, and C. Xia, "Impact of reputation assortment on tag-mediated altruistic behaviors in the spatial lattice," Appl. Math. Comput. **396**, 125928 (2021).
[38]X. Li, S. Sun, and C. Xia, "Reputation-based adaptive adjustment of link weight among individuals promotes the cooperation in spatial social dilemmas," Appl. Math. Comput. **361**, 810–820 (2019).

[39]Q. Su, A. Li, and L. Wang, "Evolutionary dynamics under interactive diversity," New J. Phys. **19**, 103023 (2017).
[40]F. C. Santos, M. D. Santos, and J. M. Pacheco, "Social diversity promotes the emergence of cooperation in public goods games," Nature **454**, 213–216 (2008).
[41]X. Chen and L. Wang, "Promotion of cooperation induced by appropriate payoff aspirations in a small-world networked game," Phys. Rev. E **77**, 017103 (2008).
[42]M. Perc and Z. Wang, "Heterogeneous aspirations promote cooperation in the prisoner's dilemma game," PLoS One **5**, e15117 (2010).
[43]J. Vukov, G. Szabó, and A. Szolnoki, "Cooperation in the noisy case: Prisoner's dilemma game on two types of regular random graphs," Phys. Rev. E **73**, 067103 (2006).
[44]U. Alvarez-Rodriguez, F. Battiston, G. F. de Arruda, Y. Moreno, M. Perc, and V. Latora, "Evolutionary dynamics of higher-order interactions in social networks," Nat. Hum. Behav. **5**, 586–595 (2021).
[45]M. Chen, L. Wang, S. Sun, J. Wang, and C. Xia, "Evolution of cooperation in the spatial public goods game with adaptive reputation assortment," Phys. Lett. A **380**, 40–47 (2016).
[46]Q. Su, A. Li, L. Wang, and H. Eugene Stanley, "Spatial reciprocity in the evolution of cooperation," Proc. R. Soc. B **286**, 20190041 (2019).
[47]Q. Su, A. McAvoy, L. Wang, and M. A. Nowak, "Evolutionary dynamics with game transitions," Proc. Natl. Acad. Sci. U.S.A. **116**, 25398–25404 (2019).
[48]A. Matsui, "Best response dynamics and socially stable strategies," J. Econ. Theor. **57**, 343–362 (1992).
[49]M. Sysi-Aho, J. Saramäki, J. Kertész, and K. Kaski, "Spatial snowdrift game with myopic agents," Eur. Phys. J. B **44**, 129–135 (2005).
[50]X. Chen and L. Wang, "Cooperation enhanced by moderate tolerance ranges in myopically selective interactions," Phys. Rev. E **80**, 046109 (2009).
[51]C. P. Roca, J. A. Cuesta, and A. Sánchez, "Promotion of cooperation on networks? The myopic best response case," Eur. Phys. J. B **71**, 587–595 (2009).
[52]G. Szabo, A. Szolnoki, M. Varga, and L. Hanusovszky, "Ordering in spatial evolutionary games for pairwise collective strategy updates," Phys. Rev. E **82**, 026110 (2010).
[53]G. Szabo and A. Szolnoki, "Selfishness, fraternity, and other-regarding preference in spatial evolutionary games," J. Theor. Biol. **299**, 81–87 (2012).
[54]G. Szabo, A. Szolnoki, and L. Czako, "Coexistence of fraternity and egoism for spatial social dilemmas," J. Theor. Biol. **317**, 126–132 (2013).
[55]A. Szolnoki and M. Perc, "Evolution of extortion in structured populations," Phys. Rev. E **89**, 022804 (2014).
[56]G. Szabó and A. Szolnoki, "Congestion phenomena caused by matching pennies in evolutionary games," Phys. Rev. E **91**, 032110 (2015).
[57]M. A. Amaral and M. A. Javarone, "Heterogeneous update mechanisms in evolutionary games: Mixing innovative and imitative dynamics," Phys. Rev. E **97**, 042305 (2018).
[58]J. Vukov, F. C. Santos, and J. M. Pacheco, "Cognitive strategies take advantage of the cooperative potential of heterogeneous networks," New J. Phys. **14**, 063031 (2012).
[59]C. Hauert and M. Doebeli, "Spatial structure often inhibits the evolution of cooperation in the snowdrift game," Nature **428**, 643–646 (2004).
[60]M. A. Amaral, M. Perc, L. Wardil, A. Szolnoki, E. J. da Silva Júnior, and J. K. da Silva, "Role-separating ordering in social dilemmas controlled by topological frustration," Phys. Rev. E **95**, 032307 (2017).
[61]C. P. Roca, J. A. Cuesta, and A. Sánchez, "Effect of spatial structure on the evolution of cooperation," Phys. Rev. E **80**, 046106 (2009).
[62]J. Tanimoto, "Difference of reciprocity effect in two coevolutionary models of presumed two-player and multiplayer games," Phys. Rev. E **87**, 062136 (2013).
[63]J. Tanimoto, "Promotion of cooperation by payoff noise in a 2 × 2 game," Phys. Rev. E **76**, 041130 (2007).
[64]G. Szabó and G. Bunth, "Social dilemmas in multistrategy evolutionary potential games," Phys. Rev. E **97**, 012305 (2018).